Side Information Effect on Semi-Blind Channel Identification for MIMO-OFDM Communications Systems

Ouahbi Rekik, Anissa Mokraoui
L2TI, UR 3043,
Université Sorbonne Paris Nord
firstname.name@univ-paris13.fr

Tran Thi Thuy Quynh
VNU University of Engineering and Technology
quynhttt@vnu.edu.vn

Trung-Thanh Le, Karim Abed-Meraim
PRISME Lab.
Université d'Orléans
firstname.name@univ-orleans.fr

***Abstract*—This paper investigates the impact of different priors, related to communications channels, on semi-blind channel estimation performance for Multiple-Input Multiple-Output Orthogonal Frequency Division Multiplexing (MIMO-OFDM) communications systems. For an estimator-independent study, the Cramér-Rao Bound (CRB) is considered to analyze the performance limits and to quantify the channel estimation gain obtained by properly exploiting side information about the propagation channel. The analysis is carried out by considering three cases: (i) no modeling while estimating the channel coefficients in the frequency domain (for each frequency bin); (ii) a finite memory linear time invariant channel model while estimating the channel taps in the time domain; and finally (iii) a specular channel model while estimating the propagation channel parameters, i.e. the fading, the delay and the angle of arrival of each path. In the latter case, the impact of a model misspecification (caused for example by array calibration errors) on the channel estimation performance is investigated by using the misspecified CRB (MCRB).**

***Index Terms*—CRB, MCRB, MIMO-OFDM, semi-blind channel identification, side information, specular channel model.**

I. Introduction

Channel State Information (CSI) remains a current concern in Multiple-Input Multiple-Output Orthogonal Frequency Division Multiplexing (MIMO-OFDM) wireless communications systems, since the system's overall performance depends strongly on it [1]. Several channel estimation approaches have been proposed in literature, mainly pilot based and blind techniques. In general, pilot-based channel estimators, which rely on some pilots inserted in the transmitted frames as specified in most communications standards [2], [3], provide an easier and more accurate channel estimation, but leads to decreasing the spectral efficiency and the throughput as compared to the blind methods (e.g. [4]–[6]), which require big amount of data. Consequently, it would be advantageous to benefit from the two strategies where both data and pilots are exploited through a semi-blind estimation approach [7]–[9].

Besides known data or statistical information, some priors (or side information) on the communications system can be available and can therefore affect the performance of the channel estimation.

Consequently, this paper aims to study the impact of different priors, relative to the channel, on a MIMO-OFDM system identification performance when adopting semi-blind approaches. To do so, Cramèr-Rao Bound (CRB) is used to quantify the performance limits independently of the estimator. Furthermore, a comparative study is conducted by considering three cases. The first case concerns the estimation of the channel fading coefficients in the frequency domain (for each frequency bin) disregarding its (finite memory) time domain structure. In the second case, a finite impulse response (FIR) linear time-invariant channel model is considered and the channel taps are estimated in the time domain. In the third case, a specular channel model is considered and the propagation channel parameters, i.e. the fading, the delay and the angle of arrival of each path are estimated. It is worth pointing out that authors in [7] carried out a through study on the CRB derivation when only considering the channel taps estimation in time domain. In the current work; and as an extension of the previous work, a comparative study of the performance gain is conducted by considering also the CRB derivation for estimating the channel coefficients in the frequency domain as well as the CRB for estimating the propagation channel parameters (i.e. the fading, the delay and the angle of arrival of each path) corresponding to a specular channel model. Furthermore, we will investigate the impact of a model misspecification on the specular channel estimation performance using the MCRB, which provides performance lower bounds for semi-blind channel estimation techniques under model misspecification.

II. MIMO-OFDM Communications System Model

The MIMO-OFDM communications system considered in this paper is represented by N_t mono-antenna transmitters and a receiver equipped with N_r receive antennas. Each transmitted OFDM symbol is composed of K samples extended by the insertion of a Cyclic Prefix (CP) corresponding to the last L samples at the beginning of the OFDM symbol, so that the CP length is assumed to be greater than or equal to the maximum channel delay denoted N (i.e. $N \leq L$). Once removing the CP and taking the K-point FFT of the received OFDM symbols, the received signal (of size K) at the N_r antennas can be expressed either in frequency or time domain by [10]:

$$\mathbf{y} = \boldsymbol{\lambda}\mathbf{x} + \mathbf{v} = \bar{\mathbf{X}}\boldsymbol{\Lambda} + \mathbf{v} = \tilde{\mathbf{X}}\mathbf{h} + \mathbf{v}, \quad (1)$$

where $\mathbf{y} = \left[\mathbf{y}_1^T \cdots \mathbf{y}_{N_r}^T\right]^T$; $\mathbf{x} = \left[\mathbf{x}_1^T \cdots \mathbf{x}_{N_t}^T\right]^T$; $\mathbf{v} = \left[\mathbf{v}_1^T \cdots \mathbf{v}_{N_r}^T\right]^T$; and $\boldsymbol{\lambda} = [\boldsymbol{\lambda}_1 \cdots \boldsymbol{\lambda}_{N_t}]$ with $\boldsymbol{\lambda}_i = [\boldsymbol{\lambda}_{i,1} \cdots \boldsymbol{\lambda}_{i,N_r}]^T$ where $\boldsymbol{\lambda}_{i,r} = diag\{\mathbf{W}\mathbf{h}_{i,r}\}$, so that $\mathbf{W}$ is a matrix containing the N first columns of an $K \times K$ Fourier transform and $\mathbf{h}_{i,r} = [h_{i,r}(0), \cdots, h_{i,r}(N-1)]^T$ contains the channel taps between the i-th transmitter and the r-th receive antenna. $\boldsymbol{\Lambda} = \left[\bar{\boldsymbol{\lambda}}_{1,1}^T \cdots \bar{\boldsymbol{\lambda}}_{i,r}^T \cdots \bar{\boldsymbol{\lambda}}_{N_t,N_r}^T\right]^T$, which is a $KN_rN_t \times 1$ vector with $\bar{\boldsymbol{\lambda}}_{i,r} = \mathbf{W}\mathbf{h}_{i,r}$ of size $K \times 1$. $\bar{\mathbf{X}} = [\mathbf{I}_{N_r} \otimes \mathbf{x}_1 ... \mathbf{I}_{N_r} \otimes \mathbf{x}_{N_t}]$. $\mathbf{h} = \left[\mathbf{h}_1^T \cdots \mathbf{h}_{N_r}^T\right]^T$ is a vector of size $N_rN_tN \times 1$ where $\mathbf{h}_r = \left[\mathbf{h}_{1,r}^T \cdots \mathbf{h}_{N_t,r}^T\right]^T$. $\tilde{\mathbf{X}} = \mathbf{I}_{N_r} \otimes \mathbf{X}$ is a matrix of size $N_rK \times NN_tN_r$ with $\otimes$ being the Kronecker product and $\mathbf{X} = \left[\mathbf{X}_{D_1}\mathbf{W} \cdots \mathbf{X}_{D_{N_t}}\mathbf{W}\right]$ of size $K \times NN_t$; where $\mathbf{X}_{D_i} = diag\{\mathbf{x}_i\}$ is a diagonal matrix of size $K \times K$.

Furthermore, some priors on the channel impulse response and/or on the communications system can be available. Hence, by assuming a specular channel model in our case, the communications channel impulse response, of the i-th user, is expressed as a function of the fading, the delay and the Direction Of Arrival (DOA), in time domain, as follows:

$$\mathbf{h}_i(t) = \sum_{l=1}^{M} \bar{h}_{i,l}\mathbf{a}(\alpha_{i,l}) sinc(t - \tau_{i,l}), \quad (2)$$

where M is the number of paths for each transmitter, $\bar{h}_{i,l}$ is the complex fading related to the l-th path, $\tau_{i,l}$ being the l-th path delay and $\mathbf{a}(\alpha_{i,l}) = \left[1\ e^{-j2\pi\frac{d}{\lambda}cos(\alpha_{i,l})} \ldots e^{-j2\pi\frac{d}{\lambda}(r-1)cos(\alpha_{i,l})} \ldots e^{-j2\pi\frac{d}{\lambda}(N_r-1)cos(\alpha_{i,l})}\right]^T$ is the steering vector with $\alpha_{i,l}$ being the corresponding DOA[1]; while λ and d represent respectively the wave length and the distance separating two adjacent receive antennas.

III. CRB DERIVATION

In what follows, the derivation of the CRB for the three considered cases is performed.

A. Considering frequency-domain and time-domain channel coefficients

This section is dedicated to the CRB derivation for frequency-domain and the time-domain channel coefficients estimation. Basically, the CRB is obtained as the inverse of the Fisher Information Matrix (FIM) denoted by $\mathbf{J}_{\boldsymbol{\theta\theta}}$ where $\boldsymbol{\theta}$ is the unknown parameters vector to be estimated [11].

By taking into account the pilots and data (that are statistically independent) in a semi-blind fashion, the total FIM is expressed as follows:

$$\mathbf{J}_{\boldsymbol{\theta\theta}} = \mathbf{J}_{\boldsymbol{\theta\theta}}^p + \mathbf{J}_{\boldsymbol{\theta\theta}}^d, \quad (3)$$

where $\mathbf{J}_{\boldsymbol{\theta\theta}}^p$ is the FIM associated to the known pilots while $\mathbf{J}_{\boldsymbol{\theta\theta}}^d$ is related to the unknown data.

Under the assumption of known signal and noise powers[2], the parameters vector to be estimated is given by:

$$\boldsymbol{\theta} = [\boldsymbol{\beta}^T \ \ (\boldsymbol{\beta}^*)^T]^T, \quad (4)$$

where

$$\boldsymbol{\beta} = \begin{cases} \boldsymbol{\Lambda} & \text{for the frequency-domain channel coefficients} \\ \mathbf{h} & \text{for the time-domain channel coefficients} \end{cases} \quad (5)$$

1) Pilot-based CRB derivation: By considering only pilots and since the noise is an i.i.d. random process, the FIM when considering N_p pilot OFDM symbols can be expressed as follows:

$$\mathbf{J}_{\boldsymbol{\theta\theta}}^p = \sum_{i=1}^{N_p} \mathbf{J}_{\boldsymbol{\theta\theta}}^{p_i}, \quad (6)$$

where $\mathbf{J}_{\boldsymbol{\theta\theta}}^{p_i}$, which refers to the FIM associated to the i-th pilot OFDM symbol, is given by:

$$\begin{aligned} \mathbf{J}_{\boldsymbol{\theta\theta}}^{p_i} &= E\left\{\left(\frac{\partial \ln p(\mathbf{y}(i), \boldsymbol{\beta})}{\partial \boldsymbol{\theta}^*}\right)\left(\frac{\partial \ln p(\mathbf{y}(i), \boldsymbol{\beta})}{\partial \boldsymbol{\theta}^*}\right)^H\right\} \\ &= \begin{pmatrix} \mathbf{J}_{\boldsymbol{\beta\beta}}^{p_i} & \mathbf{0} \\ \mathbf{0} & \mathbf{J}_{\boldsymbol{\beta^*\beta^*}}^{p_i} \end{pmatrix}. \end{aligned} \quad (7)$$

with $E(.)$ being the expectation operator and $p(\mathbf{y}(i), \boldsymbol{\beta})$ is the probability density function of the received signal given $\boldsymbol{\beta}$ and $\mathbf{J}_{\boldsymbol{\beta^*\beta^*}}^{p_i} = (\mathbf{J}_{\boldsymbol{\beta\beta}}^{p_i})^*$.

Hence, for the frequency-domain and the time-domain channel coefficients respectively, one could show that:

$$\mathbf{J}_{\boldsymbol{\theta\theta}}^{p_i} = \begin{cases} \frac{\bar{\mathbf{X}}(i)^H\bar{\mathbf{X}}(i)}{\sigma_{\mathbf{v}}^2} & \text{frequency-domain representation,} \\ \frac{\tilde{\mathbf{X}}(i)^H\tilde{\mathbf{X}}(i)}{\sigma_{\mathbf{v}}^2} & \text{time-domain representation.} \end{cases} \quad (8)$$

Finally, the pilot-based CRB is obtained as the inverse of $\mathbf{J}_{\boldsymbol{\theta\theta}}^p$.

2) Semi-blind CRB derivation: For the semi-blind channel estimation case, we assume that the data symbols are i.i.d. circular Gaussian distributed with zero mean and a diagonal covariance matrix composed of the users' transmit powers i.e. $\mathbf{C}_{\mathbf{x}} = diag\left(\boldsymbol{\sigma}_{\mathbf{x}}^2\right)$ with $\boldsymbol{\sigma}_{\mathbf{x}}^2 \overset{\text{def}}{=} \left[\sigma_{\mathbf{x}_1}^2 \cdots \sigma_{\mathbf{x}_{N_t}}^2\right]^T$ where $\sigma_{\mathbf{x}_i}^2$ denotes the transmit power of the i-th user. Under this assumption, the received signal $\mathbf{y}$ is circular Gaussian with covariance matrix:

$$\mathbf{C}_{\mathbf{y}} = \sum_{i=1}^{N_t} \sigma_{\mathbf{x}_i}^2 \boldsymbol{\lambda}_i \boldsymbol{\lambda}_i^H + \sigma_{\mathbf{v}}^2 \mathbf{I}_{KN_r}. \quad (9)$$

The total data FIM has the following form:

$$\mathbf{J}_{\boldsymbol{\theta\theta}}^d = N_d \begin{bmatrix} \mathbf{J}_{\boldsymbol{\beta\beta}}^d & \mathbf{J}_{\boldsymbol{\beta\beta^*}}^d \\ \mathbf{J}_{\boldsymbol{\beta^*\beta}}^d & \mathbf{J}_{\boldsymbol{\beta^*\beta^*}}^d \end{bmatrix} \quad (10)$$

where the elements of $\mathbf{J}_{\boldsymbol{\beta\beta}}^d$ are given by:

$$J_{\beta_i\beta_j}^d = tr\left\{\mathbf{C}_{\mathbf{y}}^{-1}\frac{\partial \mathbf{C}_{\mathbf{y}}}{\partial \beta_i^*}\mathbf{C}_{\mathbf{y}}^{-1}\left(\frac{\partial \mathbf{C}_{\mathbf{y}}}{\partial \beta_j^*}\right)^H\right\}. \quad (11)$$

with $\frac{\partial \mathbf{C}_{\mathbf{y}}}{\partial h_i^*} = \boldsymbol{\lambda}\mathbf{C}_{\mathbf{x}}\frac{\partial \boldsymbol{\lambda}^H}{\partial h_i^*}$.

[1]For simplicity, we assumed that the receive antenna corresponds to a uniform linear array.

[2]The case of unknown noise and signal powers leads to similar conclusions and is omitted here for simplicity.

Once the total FIM $\mathbf{J}_{\boldsymbol{\theta\theta}}$ is obtained as in (3), it is inverted to obtain the CRB matrix. Then, the top-left $KN_tN_r \times KN_tN_r$ (respectively $NN_tN_r \times NN_tN_r$) subblock of the CRB matrix is extracted to deduce the CRB for the subcarrier (respectively time-domain) channel coefficients estimation.

B. Considering specular channel model

This section derives the CRB of semi-blind channel estimation when considering a specular model for the channel impulse response as given in equation (2). Thus, the vector parameter of size $4NN_rN_t \times 1$ to be estimated is given by:

$$\boldsymbol{\theta} = [\bar{\boldsymbol{h}}^T \ \ (\bar{\boldsymbol{h}}^*)^T \ \ \boldsymbol{\tau}^T \ \ \boldsymbol{\alpha}^T]^T, \tag{12}$$

with $\bar{\boldsymbol{h}}, \boldsymbol{\tau}, \boldsymbol{\alpha}$ being vectors of size $NN_rN_t \times 1$ containing respectively the complex fading, the delay and the DOA of channel taps between all users and the receive antennas.

According to the FIM derivation of parameter transformation [11], the FIM in such a case is based on that derived in section III-A. Thus, by denoting $\mathbf{J}^{\mathbf{h}}_{\boldsymbol{\theta\theta}}$ the FIM of the semi-blind time-domain channel coefficients estimation, we have:

$$\mathbf{J}_{\boldsymbol{\theta\theta}} = \frac{\partial \mathbf{h}}{\partial \boldsymbol{\theta}}^H \mathbf{J}^{\mathbf{h}}_{\boldsymbol{\theta\theta}} \frac{\partial \mathbf{h}}{\partial \boldsymbol{\theta}}, \quad \text{where} \quad \frac{\partial \mathbf{h}}{\partial \boldsymbol{\theta}} = \Big[\frac{\partial \mathbf{h}}{\partial \bar{\boldsymbol{h}}}, \frac{\partial \mathbf{h}}{\partial \bar{\boldsymbol{h}}^*}, \frac{\partial \mathbf{h}}{\partial \boldsymbol{\tau}}, \frac{\partial \mathbf{h}}{\partial \boldsymbol{\alpha}}\Big], \tag{13}$$

More precisely, we have:

$$\frac{\partial \mathbf{h}}{\partial \bar{\mathbf{h}}} = \big[\mathbf{B}_1^\top, \ \ \mathbf{B}_2^\top, \ \ \ldots, \ \ \mathbf{B}_{N_r}^\top\big], \tag{14}$$

$$\mathbf{B}_r = \operatorname{diag}([\mathbf{B}_{1,r}, \ \mathbf{B}_{2,r}, \ \ldots, \ \mathbf{B}_{N_t,r}]), \tag{15}$$

$$\mathbf{B}_{i,r} = \begin{bmatrix} \frac{\partial h_{i,r}(0)}{\partial \bar{h}_{i,1}} & \frac{\partial h_{i,r}(1)}{\partial \bar{h}_{i,1}} & \cdots & \frac{\partial h_{i,r}(N-1)}{\partial \bar{h}_{i,1}} \\ \frac{\partial h_{i,r}(0)}{\partial \bar{h}_{i,2}} & \frac{\partial h_{i,r}(1)}{\partial \bar{h}_{i,2}} & \cdots & \frac{\partial h_{i,r}(N-1)}{\partial \bar{h}_{i,2}} \\ \vdots & \vdots & \cdots & \vdots \\ \frac{\partial h_{i,r}(0)}{\partial \bar{h}_{i,M}} & \frac{\partial h_{i,r}(1)}{\partial \bar{h}_{i,M}} & \cdots & \frac{\partial h_{i,r}(N-1)}{\partial \bar{h}_{i,M}} \end{bmatrix}, \tag{16}$$

The derivatives $\frac{\partial \mathbf{h}}{\partial \tau}$ and $\frac{\partial \mathbf{h}}{\partial \alpha}$ are performed in the same way as $\partial \mathbf{h}/\partial \bar{\mathbf{h}}$, but respectively with the following elements:

$$\begin{aligned} \frac{\partial h_{i,r}(t)}{\partial \tau_{i,l}} &= \bar{h}_{i,l}\left(\frac{\sin(t-\tau_{i,l})}{(t-\tau_{i,l})^2} - \frac{\cos(l-\tau_{i,l})}{t-\tau_{i,l}}\right) \\ &\quad \times \exp\left(-i2\pi\frac{d}{\lambda}(r-1)\sin(\alpha_{m,i})\right), \end{aligned} \tag{17}$$

$$\begin{aligned} \frac{\partial h_{i,r}(l)}{\partial \alpha_{i,l}} &= \bar{h}_{i,l}\operatorname{sinc}(t-\tau_{i,l})\frac{-i2\pi d(r-1)\cos(\alpha_{l,i})}{\lambda} \\ &\quad \times \exp\left(-i2\pi\frac{d}{\lambda}(r-1)\sin(\alpha_{i,l})\right). \end{aligned} \tag{18}$$

IV. MCRB FOR SPECULAR CHANNEL MODEL

In practice, the channel model given by (2) can be potentially misspecified due to the propagation model itself or to array calibration errors which affect the channel estimation accuracy. Consequently, this section is dedicated to analysis the impact of such errors on the channel estimation performance and therefor, to determine to which extent one can rely on such a model and preserve its advantage over the simple FIR model.

To do so, the basic tool will be the misspecified CRB (MCRB) which is an extension of the usual CRB for dealing with model misspecifications [12].

A. Brief review of MCRB

Hence, if we assume that the received data samples are i.i.d. derived from the true pdf denoted by $f(\mathbf{y})$, then, under a mismatched estimation, instead of $f(\mathbf{y})$, users adopt a different pdf denoted by $\tilde{f}(\mathbf{y}|\boldsymbol{\theta})$ where $\tilde{f}(\mathbf{y}|\boldsymbol{\theta}) \neq f(\mathbf{y}) \ \forall \boldsymbol{\theta}$ is allowed. Thus, for the users, the problem of interest is now to estimate $\boldsymbol{\theta}$.

In the context of MCRB, Kullback-Leibler (KL) divergence is used to determine the "best" performance that can be achieved by unbiased estimators under model misspecification. It is defined as:

$$\mathrm{KL}\left(f \parallel \tilde{f}\right) \triangleq E_f\{\log f(\mathbf{y})\} - E_f\{\log \tilde{f}(\mathbf{y}|\boldsymbol{\theta})\}. \tag{19}$$

The unique minimizer of $\mathrm{KL}(f \parallel \tilde{f})$ is called the *pseudo-true* parameter denoted by $\boldsymbol{\theta}_{pt}$. In fact, minimizing (19) is equivalent to maximizing $E_f\{\log \tilde{f}(\mathbf{y}|\boldsymbol{\theta})\}$:

$$\boldsymbol{\theta}_{pt} \triangleq \underset{\boldsymbol{\theta}}{\operatorname{argmin}}\, \mathrm{KL}\left(f \parallel \tilde{f}\right) = \underset{\boldsymbol{\theta}}{\operatorname{argmax}}\, E_f\{\ell(\mathbf{y}|\boldsymbol{\theta})\}, \tag{20}$$

where $\ell(\mathbf{y}|\boldsymbol{\theta}) \triangleq \log\, \tilde{f}(\boldsymbol{y}|\boldsymbol{\theta})$.

Accordingly, the maximum likelihood estimator (MLE) converges in probability to $\boldsymbol{\theta}_{pt}$ [13]–[15].

Let $\hat{\boldsymbol{\theta}}$ be an estimator derived under the misspecified model $\tilde{f}(\boldsymbol{y}|\boldsymbol{\theta})$ from the output samples. We call $\hat{\boldsymbol{\theta}}$ as misspecified (MS)-unbiased estimator if and only if:

$$E_f\{\hat{\boldsymbol{\theta}}(\boldsymbol{y})\} = \int \hat{\boldsymbol{\theta}}(\boldsymbol{y}) f(\boldsymbol{y}) d\boldsymbol{y} = \boldsymbol{\theta}_{pt}. \tag{21}$$

Whereas, the its covariance matrix is so that:[3]

$$\mathrm{VAR}\left(\hat{\boldsymbol{\theta}}\right) \geq \mathrm{MCRB}(\boldsymbol{\theta}_{pt}) \triangleq \boldsymbol{A}^{\#}(\boldsymbol{\theta}_{pt}) \boldsymbol{J}(\boldsymbol{\theta}_{pt}) \boldsymbol{A}^{\#}(\boldsymbol{\theta}_{pt}), \tag{22}$$

where $(.)^{\#}$ denotes the pseudo-inverse operator and the two matrices $\boldsymbol{J}(\boldsymbol{\theta})$ and $\boldsymbol{A}(\boldsymbol{\theta})$ are defined as follows:

$$\boldsymbol{J}(\boldsymbol{\theta}) = E_f\left\{\frac{\partial \ell}{\partial \boldsymbol{\theta}^*}\left(\frac{\partial \ell}{\partial \boldsymbol{\theta}^*}\right)^H\right\}, \ \boldsymbol{A}(\boldsymbol{\theta}) = E_f\left\{\frac{\partial}{\partial \boldsymbol{\theta}}\left(\frac{\partial \ell}{\partial \boldsymbol{\theta}^*}\right)\right\}. \tag{23}$$

B. MCRB derivation for erroneous number of multipaths

This subsection is devoted to the derivation of the MCRB of unbiased channel estimators when the multipath is misspecified.

According to the system model given by (1), the true joint pdf function $f(\boldsymbol{y}_p, \boldsymbol{y}_d|\boldsymbol{\theta})$ can be expressed as follows:

$$\begin{aligned} f(\boldsymbol{y}_p, \boldsymbol{y}_d|\boldsymbol{\theta}) &= \prod_{n=1}^{N_p} \frac{1}{(\pi\sigma_v^2)^{N_rK}} \exp\left(-\frac{1}{\sigma_v^2}\left\|\boldsymbol{y}_p(n) - \boldsymbol{m}_p(n)\right\|_2^2\right) \\ &\quad \times \prod_{n=1}^{N_d} \frac{1}{\pi^{N_rK}\det \boldsymbol{C}_y} \exp\left(-\boldsymbol{y}_d(n)^H \boldsymbol{C}_y^{-1} \boldsymbol{y}_d(n)\right), \end{aligned} \tag{24}$$

where $\boldsymbol{m}_p(n) = \boldsymbol{\lambda}\boldsymbol{x}_p(n) = \tilde{\boldsymbol{X}}_p(n)\boldsymbol{h}$.

[3]In regular problems, the generalized interpretation of the MCRB in (22) boils down to the usual one

$$\mathrm{MCRB}(\boldsymbol{\theta}_{pt}) \triangleq \boldsymbol{A}^{-1}(\boldsymbol{\theta}_{pt}) \boldsymbol{J}(\boldsymbol{\theta}_{pt}) \boldsymbol{A}^{-1}(\boldsymbol{\theta}_{pt}).$$

However, due to the imperfect knowledge of M, the users use the following assumed pdf function:

$$\begin{aligned}\tilde{f}\big(\boldsymbol{y}_p,\boldsymbol{y}_d|\boldsymbol{\theta}'\big) &= \prod_{n=1}^{N_p}\frac{1}{(\pi\sigma_v^2)^{N_rK}}\exp\left(-\frac{1}{\sigma_v^2}\big\|\boldsymbol{y}_p(n)-\tilde{\boldsymbol{m}}_p(n)\big\|_2^2\right)\\ &\times\prod_{n=1}^{N_d}\frac{1}{\pi^{N_rK}\det\tilde{\boldsymbol{C}}_y}\exp\left(-\boldsymbol{y}_d(n)^H\tilde{\boldsymbol{C}}_y^{-1}\boldsymbol{y}_d(n)\right)\\ &\triangleq \tilde{f}_p(\boldsymbol{y}_p|\boldsymbol{\theta}')\tilde{f}_d(\boldsymbol{y}_d|\boldsymbol{\theta}'),\end{aligned}\tag{25}$$

where $\tilde{\boldsymbol{m}}_p(n)$ and $\tilde{\boldsymbol{C}}_y$ are defined by using the erroneous number of multipaths.

Accordingly, the misspecified log-likehood function is then given by:

$$\ell\big(\boldsymbol{y}_p,\boldsymbol{y}_d|\boldsymbol{\theta}'\big)\triangleq\log\left(\tilde{f}\big(\boldsymbol{y}_p,\boldsymbol{y}_d|\boldsymbol{\theta}'\big)\right)=\ell_p(\boldsymbol{y}_p|\boldsymbol{\theta}')+\ell_d\big(\boldsymbol{y}_d|\boldsymbol{\theta}'\big),$$

with

$$\ell_p(\boldsymbol{y}_p|\boldsymbol{\theta}') = -N_rN_pK\log(\pi\sigma_v^2)-\sum_{n=1}^{N_p}\frac{1}{\sigma_v^2}\big\|\boldsymbol{y}_p(n)-\tilde{\boldsymbol{m}}_p(n)\big\|_2^2,$$

$$\ell_d\big(\boldsymbol{y}_d|\boldsymbol{\theta}'\big) = -\sum_{n=1}^{N_d}\log\left(\pi^{PN}\det\tilde{\boldsymbol{C}}_y\right)-\sum_{n=1}^{N_d}\boldsymbol{y}_d(n)^H\tilde{\boldsymbol{C}}_y^{-1}\boldsymbol{y}_d(n).$$

Since the *pseudo-true* parameter $\boldsymbol{\theta}_{pt}$ is derived from $\max_{\boldsymbol{\theta}'}\mathbb{E}_f\left\{\ell\big(\boldsymbol{y}_p,\boldsymbol{y}_d|\boldsymbol{\theta}'\big)\right\}$, we obtain

$$E_f\left\{\nabla\ell_p\big(\boldsymbol{y}_p|\boldsymbol{\theta}'\big)\right\}\Big|_{\boldsymbol{\theta}'=\boldsymbol{\theta}_{pt}} = -E_f\left\{\nabla\ell_d\big(\boldsymbol{y}_d|\boldsymbol{\theta}'\big)\right\}\Big|_{\boldsymbol{\theta}'=\boldsymbol{\theta}_{pt}}.\tag{26}$$

Consequently, the two factor matrices of the MCRB can be decomposed into two parts as follows:

$$\begin{aligned}\boldsymbol{J}_{\text{SB}}(\boldsymbol{\theta}') &= E_f\left\{\frac{\partial\ell_p}{\partial\boldsymbol{\theta}'^*}\left(\frac{\partial\ell_p}{\partial\boldsymbol{\theta}'^*}\right)^H\right\}+E_f\left\{\frac{\partial\ell_d}{\partial\boldsymbol{\theta}'^*}\left(\frac{\partial\ell_d}{\partial\boldsymbol{\theta}'^*}\right)^H\right\}\\ &\triangleq \boldsymbol{J}^p(\boldsymbol{\theta}')+\boldsymbol{J}^d(\boldsymbol{\theta}'),\end{aligned}\tag{27}$$

$$\begin{aligned}\boldsymbol{A}_{\text{SB}}(\boldsymbol{\theta}') &= E_f\left\{\frac{\partial}{\partial\boldsymbol{\theta}'}\left(\frac{\partial\ell_p}{\partial\boldsymbol{\theta}'^*}\right)\right\}+E_f\left\{\frac{\partial}{\partial\boldsymbol{\theta}'}\left(\frac{\partial\ell_d}{\partial\boldsymbol{\theta}'^*}\right)\right\}\\ &\triangleq \boldsymbol{A}^p(\boldsymbol{\theta}')+\boldsymbol{A}^d(\boldsymbol{\theta}'),\end{aligned}\tag{28}$$

where $\boldsymbol{J}^p(\boldsymbol{\theta}')$ and $\boldsymbol{A}^p(\boldsymbol{\theta}')$ are dedicated to $\text{MCRB}^p(\boldsymbol{\theta}')$ for the pilot symbols, while $\boldsymbol{J}^d(\boldsymbol{\theta}')$ and $\boldsymbol{A}^d(\boldsymbol{\theta}')$ concern the misspecified lower bound corresponding to the data symbols.

1) Pilot-based MCRB: Under the assumption that the noise is supposed to be i.i.d. random variables, $\boldsymbol{J}^p(\boldsymbol{\theta}')$ and $\boldsymbol{A}^p(\boldsymbol{\theta}')$ can be given by:

$$\boldsymbol{J}^p(\boldsymbol{\theta}')=\sum_{n=1}^{N_p}\boldsymbol{J}_n^p(\boldsymbol{\theta}'),\ \text{and}\ \boldsymbol{A}^p(\boldsymbol{\theta}')=\sum_{n=1}^{N_p}\boldsymbol{A}_n^p(\boldsymbol{\theta}'),\tag{29}$$

where $\boldsymbol{J}_n^p(\boldsymbol{\theta}')$ and $\boldsymbol{A}_n^p(\boldsymbol{\theta}')$ correspond to the n-th pilot OFDM symbol. In the same way, the misspecified log-likelihood function $\ell_p(\boldsymbol{y}_p|\boldsymbol{\theta}')$ is given by:

$$\ell_p\big(\boldsymbol{y}_p|\boldsymbol{\theta}'\big)=\sum_{n=1}^{N_p}\ell_n\big(\boldsymbol{y}_p(n)|\boldsymbol{\theta}'\big),\tag{30}$$

with

$$\ell_n\big(\boldsymbol{y}_p(n)|\boldsymbol{\theta}'\big)=-N_rK\log(\pi\sigma_v^2)-\frac{1}{\sigma_v^2}\big\|\boldsymbol{y}_p(n)-\tilde{\boldsymbol{m}}_p(n)\big\|_2^2,\tag{31}$$

In such a case, the vector of unknown parameters is given by $\boldsymbol{\theta}'=\left[\boldsymbol{\psi}'^\top,\sigma_v^2\right]^\top$, where $\boldsymbol{\psi}'=\left[\boldsymbol{\beta}'^\top,\boldsymbol{\alpha}'^\top,\boldsymbol{\tau}'^\top\right]^\top$. Accordingly, one could show that:

$$\boldsymbol{J}_n^p(\boldsymbol{\theta}')=\begin{bmatrix}\boldsymbol{J}_n^p(\boldsymbol{\psi}',\boldsymbol{\psi}') & \boldsymbol{J}_n^p(\boldsymbol{\psi}',\sigma_v^2)\\ \boldsymbol{J}_n^p(\sigma_v^2,\boldsymbol{\psi}') & \boldsymbol{J}_n^p(\sigma_v^2,\sigma_v^2)\end{bmatrix},\tag{32}$$

$$\boldsymbol{A}_n^p(\boldsymbol{\theta}')=\begin{bmatrix}\boldsymbol{A}_n^p(\boldsymbol{\psi}',\boldsymbol{\psi}') & \boldsymbol{A}_n^p(\boldsymbol{\psi}',\sigma_v^2)\\ \boldsymbol{A}_n^p(\sigma_v^2,\boldsymbol{\psi}') & \boldsymbol{A}_n^p(\sigma_v^2,\sigma_v^2)\end{bmatrix}.\tag{33}$$

The derivative $\ell_n(\boldsymbol{y}_p|\boldsymbol{\theta}')$ w.r.t. $\boldsymbol{\psi}'$ and σ_v^2 are given by

$$\frac{\partial\ell_n}{\partial\boldsymbol{\psi}'}=\frac{-1}{\sigma_v^2}\left(\frac{\partial\tilde{\boldsymbol{m}}_p(n)}{\partial\boldsymbol{\psi}'}\right)^H\Big(\boldsymbol{y}_p(n)-\tilde{\boldsymbol{m}}_p(n)\Big),\tag{34}$$

$$\frac{\partial\ell_n}{\partial\sigma_v^2}=\frac{1}{\sigma_v^4}\big\|\boldsymbol{y}_p(n)-\tilde{\boldsymbol{m}}_p(n)\big\|_2^2-\frac{N_rK}{\sigma_v^2},\tag{35}$$

where

$$\frac{\partial\tilde{\boldsymbol{m}}_p(n)}{\partial\boldsymbol{\psi}'}=\tilde{\boldsymbol{X}}_p(n)\left[\frac{\partial\tilde{\boldsymbol{h}}}{\partial\boldsymbol{\beta}'},\frac{\partial\tilde{\boldsymbol{h}}}{\partial\boldsymbol{\tau}'},\frac{\partial\tilde{\boldsymbol{h}}}{\partial\boldsymbol{\alpha}'}\right]\triangleq\tilde{\boldsymbol{X}}_p(n)\boldsymbol{G},\tag{36}$$

By denoting the error on the mean by $\boldsymbol{e}_p(n)=\tilde{\boldsymbol{m}}_p(n)-\boldsymbol{m}_p(n)$ and $\boldsymbol{E}_p(n)=\sigma_v^2\boldsymbol{I}_{N_rK}+\boldsymbol{e}_p(n)\boldsymbol{e}_p(n)^H$, we obtain

$$\begin{aligned}&\boldsymbol{J}_n^p(\sigma_v^2,\sigma_v^2)=-\boldsymbol{A}_n^p(\sigma_v^2,\sigma_v^2)=-\frac{N_rK}{\sigma_v^4},\\ &\boldsymbol{J}_n^p(\boldsymbol{\psi}',\sigma_v^2)=\left(\boldsymbol{J}_n^p(\boldsymbol{\psi}',\sigma_v^2)\right)^H=\boldsymbol{0},\\ &\boldsymbol{A}_n^p(\boldsymbol{\psi}',\sigma_v^2)=\left(\boldsymbol{A}_n^p(\boldsymbol{\psi}',\sigma_v^2)\right)^H=\frac{1}{\sigma_v^4}\boldsymbol{G}^H\tilde{\boldsymbol{X}}_p(n)^H\boldsymbol{e}_p(n),\\ &\boldsymbol{J}_n^p(\boldsymbol{\psi}',\boldsymbol{\psi}')=-\frac{1}{\sigma_v^4}\boldsymbol{G}^H\tilde{\boldsymbol{X}}_p(n)^H\boldsymbol{E}_p(n)\tilde{\boldsymbol{X}}_p(n)\boldsymbol{G},\\ &\boldsymbol{A}_n^p(\boldsymbol{\psi}',\boldsymbol{\psi}')=\frac{1}{\sigma_v^2}\boldsymbol{G}^H\tilde{\boldsymbol{X}}_p(n)^H\tilde{\boldsymbol{X}}_p(n)\boldsymbol{G}.\end{aligned}$$

Therefore, the MCRB_{OP} for the training-based estimation, is given by:

$$\text{MCRB}_{\text{OP}}(\boldsymbol{\theta}')=\boldsymbol{A}_{\text{OP}}^{\#}(\boldsymbol{\theta}')\boldsymbol{J}_{\text{OP}}(\boldsymbol{\theta}')\boldsymbol{A}_{\text{OP}}^{\#}(\boldsymbol{\theta}'),\tag{37}$$

where

$$\boldsymbol{J}_{\text{OP}}(\boldsymbol{\theta}')=\frac{-1}{\sigma_v^4}\begin{bmatrix}\boldsymbol{G}^H\left(\sum_{n=1}^{N_p}\tilde{\boldsymbol{X}}_p^H(n)\boldsymbol{E}\tilde{\boldsymbol{X}}_p(n)\right)\boldsymbol{G} & \boldsymbol{0}\\ \boldsymbol{0} & N_pN_rK\end{bmatrix},\tag{38}$$

$$\boldsymbol{A}_{\text{OP}}(\boldsymbol{\theta}')=\frac{1}{\sigma_v^2}\begin{bmatrix}\boldsymbol{G}^H\left(\sum_{n=1}^{N_p}\tilde{\boldsymbol{X}}_p^H(n)\tilde{\boldsymbol{X}}_p(n)\right)\boldsymbol{G} & \boldsymbol{G}^H\sum_{n=1}^{N_p}\tilde{\boldsymbol{X}}_p^H(n)\boldsymbol{e}_p(n)\\ \sum_{n=1}^{N_p}\boldsymbol{e}_p^H(n)\tilde{\boldsymbol{X}}_p(n)\boldsymbol{G} & \frac{N_pN_rK}{\sigma_v^2}\end{bmatrix}.\tag{39}$$

2) Data-based MCRB: We know that the true distribution of $\boldsymbol{y}_d(n)$ is $\mathcal{CN}(\boldsymbol{0},\boldsymbol{C}_y)$ while the users assume $\boldsymbol{y}_d(n)\sim\mathcal{CN}(\boldsymbol{0},\tilde{\boldsymbol{C}}_y)$, where $\tilde{\boldsymbol{C}}_y$ is defined as

$$\tilde{\boldsymbol{C}}_y=\sum_{j=1}^{N_t}\sigma_{x_j}^2\tilde{\boldsymbol{\lambda}}_j\tilde{\boldsymbol{\lambda}}_j^H+\sigma_v^2\boldsymbol{I}_{KN_r},\tag{40}$$

where the system matrix $\tilde{\boldsymbol{\lambda}}$ is defined as

$$\tilde{\boldsymbol{\lambda}}=\left[\tilde{\boldsymbol{\lambda}}_1,\tilde{\boldsymbol{\lambda}}_2,\ldots,\tilde{\boldsymbol{\lambda}}_{N_t}\right],\quad\tilde{\boldsymbol{\lambda}}_j=\left[\tilde{\boldsymbol{\lambda}}_{1,j},\tilde{\boldsymbol{\lambda}}_{2,j},\ldots,\tilde{\boldsymbol{\lambda}}_{N_r,j}\right]^\top,\tag{41}$$

with $\tilde{\lambda}_{r,j} = \mathrm{diag}(\ \mathrm{W}\tilde{\boldsymbol{h}}_{r,j})$.

The vector of unknown parameters becomes

$$\boldsymbol{\theta}' = \left[\boldsymbol{\psi}'^{\top}, \sigma_v^2, \boldsymbol{\sigma}_x^2\right]^{\top}.$$

The derivative of $\ell_d(\boldsymbol{y}_d|\boldsymbol{\theta}')$ is given by

$$\frac{\partial \ell_d}{\partial \theta'_i} = -N_d \operatorname{tr}\left\{\tilde{\boldsymbol{C}}^{-1}\frac{\partial \tilde{\boldsymbol{C}}}{\partial \theta'_i}\right\} + \sum_{n=1}^{N_d} \boldsymbol{y}_d(n)^H \tilde{\boldsymbol{C}}^{-1}\frac{\partial \tilde{\boldsymbol{C}}}{\partial \theta'_i}\tilde{\boldsymbol{C}}^{-1}\boldsymbol{y}_d(n),$$

where $\frac{\partial \tilde{\boldsymbol{C}}}{\partial \beta'_i} = \sigma_x^2 \tilde{\boldsymbol{\lambda}} \frac{\partial \tilde{\boldsymbol{\lambda}}^H}{\partial \tilde{\boldsymbol{h}}} \frac{\partial \tilde{\boldsymbol{h}}}{\partial \beta'_i}$, $\frac{\partial \tilde{\boldsymbol{C}}}{\partial \tau'_i} = \sigma_x^2 \tilde{\boldsymbol{\lambda}} \frac{\partial \tilde{\boldsymbol{\lambda}}^H}{\partial \tilde{\boldsymbol{h}}} \frac{\partial \tilde{\boldsymbol{h}}}{\partial \tau'_i}$, $\frac{\partial \tilde{\boldsymbol{C}}}{\partial \alpha'_i} = \sigma_x^2 \tilde{\boldsymbol{\lambda}} \frac{\partial \tilde{\boldsymbol{\lambda}}^H}{\partial \tilde{\boldsymbol{h}}} \frac{\partial \tilde{\boldsymbol{h}}}{\partial \tau_{\alpha'_i}}$, $\frac{\partial \tilde{\boldsymbol{C}}}{\sigma^2_{x_j}} = \tilde{\boldsymbol{\lambda}}_j \tilde{\boldsymbol{\lambda}}_j^H$, and $\frac{\partial \tilde{\boldsymbol{C}}}{\sigma_v^2} = \boldsymbol{I}_{N_r K}$.

At $\boldsymbol{\theta}' = \boldsymbol{\theta}_{pt}$, we obtain $\mathbb{E}_f\left\{\frac{\partial \ell_d}{\partial \theta'_i}\right\} = 0$ and hence

$$N_d \operatorname{tr}\left\{\tilde{\boldsymbol{C}}^{-1}\frac{\partial \tilde{\boldsymbol{C}}}{\partial \theta'_i}\right\} = \sum_{n=1}^{N_d} \mathbb{E}_f\left\{\boldsymbol{y}_d(n)^H \tilde{\boldsymbol{C}}^{-1}\frac{\partial \tilde{\boldsymbol{C}}}{\partial \theta'_i}\tilde{\boldsymbol{C}}^{-1}\boldsymbol{y}_d(n)\right\}.$$

Accordingly, taking the expectation of $\left\{\frac{\partial \ell_d}{\partial \theta'_i}\frac{\partial \ell_d}{\partial \theta'_j}\right\}$ and $\left\{\frac{\partial^2 \ell_d}{\partial \theta'_i \partial \theta'_j}\right\}$ over the true $f(\boldsymbol{y})$ results in

$$\begin{aligned}[\boldsymbol{J}^p(\boldsymbol{\theta}')]_{ij} &= N_d \operatorname{tr}\left\{\tilde{\boldsymbol{C}}^{-1}\frac{\partial \tilde{\boldsymbol{C}}}{\partial \theta'_i}\tilde{\boldsymbol{C}}^{-1}\boldsymbol{C}\tilde{\boldsymbol{C}}^{-1}\frac{\partial \tilde{\boldsymbol{C}}}{\partial \theta'_j}\tilde{\boldsymbol{C}}^{-1}\boldsymbol{C}\right\} \\ &+ N_d \operatorname{tr}\left\{\tilde{\boldsymbol{C}}^{-1}\frac{\partial \tilde{\boldsymbol{C}}}{\partial \theta'_i}\left(\tilde{\boldsymbol{C}}^{-1}\boldsymbol{C} - \boldsymbol{I}\right)\right\} \operatorname{tr}\left\{\tilde{\boldsymbol{C}}^{-1}\frac{\partial \tilde{\boldsymbol{C}}}{\partial \theta'_j}\left(\tilde{\boldsymbol{C}}^{-1}\boldsymbol{C} - \boldsymbol{I}\right)\right\},\end{aligned} \tag{42}$$

$$\begin{aligned}[\boldsymbol{A}^d(\boldsymbol{\theta}')]_{ij} &= -N_d \operatorname{tr}\left\{\tilde{\boldsymbol{C}}^{-1}\frac{\partial \tilde{\boldsymbol{C}}}{\partial \theta'_j}\tilde{\boldsymbol{C}}^{-1}\frac{\partial \tilde{\boldsymbol{C}}}{\partial \theta'_i}\left(\tilde{\boldsymbol{C}}^{-1}\boldsymbol{C} - \boldsymbol{I}\right)\right\} \\ &+ N_d \operatorname{tr}\left\{\tilde{\boldsymbol{C}}^{-1}\frac{\partial^2 \tilde{\boldsymbol{C}}}{\partial \theta'_j \partial \theta'_i}\left(\tilde{\boldsymbol{C}}^{-1}\boldsymbol{C} - \boldsymbol{I}\right)\right\} - N_d \operatorname{tr}\left\{\tilde{\boldsymbol{C}}^{-1}\frac{\partial \tilde{\boldsymbol{C}}}{\partial \theta'_i}\tilde{\boldsymbol{C}}^{-1}\frac{\partial \tilde{\boldsymbol{C}}}{\partial \theta'_j}\tilde{\boldsymbol{C}}^{-1}\boldsymbol{C}\right\}.\end{aligned} \tag{43}$$

V. Simulation results

To highlight the performance gain of priors on the communications channels, several simulations are performed for the different scenarios as described previously: the subcarrier channel coefficient estimation ($\mathrm{CRB}^{\lambda}_{OP}, \mathrm{CRB}^{\lambda}_{SB}$), the channel taps estimation ($\mathrm{CRB}^{\mathbf{h}}_{OP}, \mathrm{CRB}^{\mathbf{h}}_{SB}$) and the specular channel coefficients estimation ($\mathrm{CRB}^{specular}_{OP}, \mathrm{CRB}^{specular}_{SB}$) where OP stands for the pilot-based estimation; whereas SB refers to the semi-blind framework. The pilot symbols are generated according to Zadoff-Chu sequences . A 2×2 MIMO-OFDM systems is considered with $N = 4$ channel taps and $K = 64$ OFDM subcarriers. Channels fading and delay are given respectively by $[0.40.60.10.01; 0.30.90.50.3]$ and $[0.40.60.10.4; 0.30.90.50.1]$, whereas DOA are as $[\frac{\pi}{2}, \frac{\pi}{4}, \frac{\pi}{6}, \frac{\pi}{8}; \frac{\pi}{3}, \frac{\pi}{4}, \frac{\pi}{7}, \frac{\pi}{8}]$.

Fig. 1 illustrates the behavior of the normalized CRB $\left(\frac{tr\{CRB\}}{\|\mathbf{h}\|^2}\right)$ versus SNR for the three considered scenarios. Adopting a semi-blind framework helps lowering the CRB and hence performing better than pilot-based approaches. One could notice that with only one pilot symbol and few data symbols (40 in our case), the efficiency of the semi-blind framework is well illustrated while preserving a lower overhead. On the other hand, one notices that compared to the frequency domain, estimating directly the channel taps in time domain gives much better performance, which is further enhanced when considering a parametric propagation model for the communications channel (specular representation in our case).

Fig. 2a illustrates the semi-blind CRB behavior of the channel coefficients estimation in frequency ($\mathrm{CRB}^{\lambda}_{\mathrm{SB}}$) and time ($\mathrm{CRB}^{\mathbf{h}}_{\mathrm{SB}}$) domain w.r.t. to the number of pilot symbols N_p. It can be noticed that, in order to reach same performance as the semi-blind CRB for specular channel estimation($\mathrm{CRB}^{specular}_{\mathrm{SB}}$) with one pilot symbol, one needs around 60 pilot symbols when estimating the channel coefficients in time domain and, seemingly, even much more when directly estimating the frequency coefficients.

Fig. 2b assesses the effect of the number of data symbols N_d on the semi-blind CRBs. One could notice that with just tens of data symbols, the semi-blind channel estimation is further enhanced, when considering the channel parameters. Also, it is noticed that the CRB curves tends to flatten with high number of data symbols, which indicates that only a reasonable number of data symbols is needed for better channel estimation performance.

Fig. 3a plots the MCRBs versus SNR when the number of multipaths is underspecified. It can be seen that the MCRBs tend to converge towards error levels as SNR increases, which is caused probably by a nonzero error mean between the true and the assumed one. It suggests that the performance of channel estimators can not exceed a deterministic threshold even when SNR goes to infinity. By contrast, the classical CRBs are approximately proportional to the noise variance which do not reflect the true performance bounds of channel estimators under model misspecification. Again, besides the performance gain obtained with semi-blind techniques, compared to pilot-based ones, one can notice that exploiting the prior specular parameters (DOA, time delay and fading) will gain the theoretical performance limit of channel estimators despite they are underspecified. Indeed, such information can be seen as constraints imposed on the channel taps, hence the resulting $(\mathrm{M})\mathrm{CRB}^{specular}$ can be referred to as a constrained $(\mathrm{M})\mathrm{CRB}$ which is often lower than the unconstrained bound.

Fig. 3b illustrates the performance lower bounds when the specular components are overspecified. In fact, the overspecification is not really a case of misspecification, as indicated in [16] and as the proposed MCRBs follow the classical CRBs in such a case.

VI. Conclusion

This paper focused on the effect of side information on the performance of semi-blind channel estimation; when considering MIMO-OFDM communications systems. Three scenarios have been investigated, estimating: (i) the channel fading coefficients in the frequency domain; (ii) the channel taps in the time domain; and (iii) the propagation channel parameters when considering a specular channel model. To quantify and compare their performance limits, CRBs have been derived. This comparative analysis reveals the superiority of the specular channel model as compared to the two others. Besides, we analyze the performance loss, due to a mismatch, on the specular channel model. Such an analysis helps to

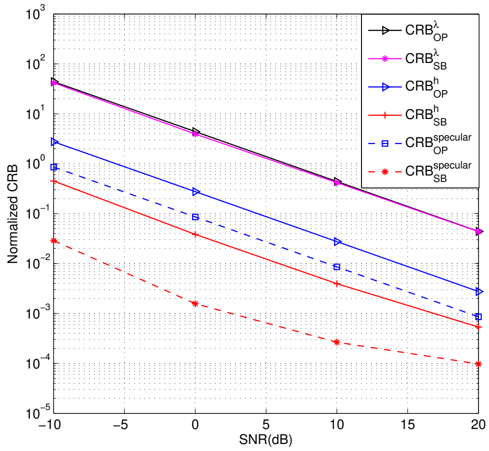

Fig. 1: Normalized pilot-based and semi-blind CRBs vs SNR, for frequency-domain, time-domain and specular channel estimation.

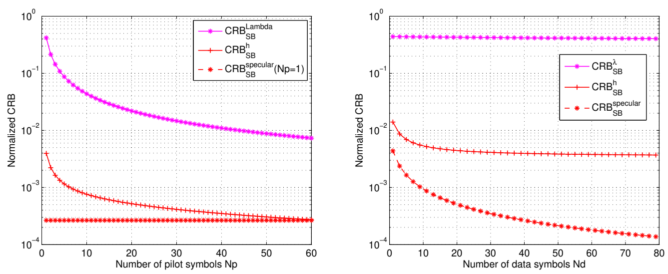

(a) (b)

Fig. 2: Normalized CRB vs (a) number of pilot symbols, and (b) number of data symbols.

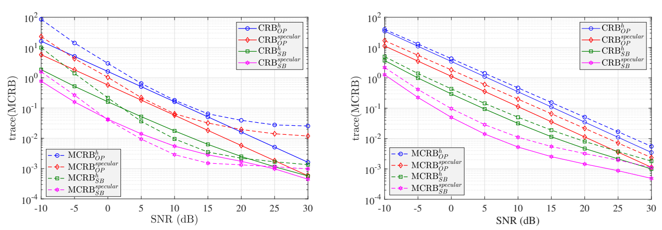

(a) (b)

Fig. 3: Proposed MCRB bounds for semi-blind channel estimation : (a) $M' = 3 < M = 4$, (b) $M' = 5 > M = 4$.

determine the error level that can be tolerated on the specular model mismatch; in order to preserve its related advantage in terms of channel estimation accuracy.

References

[1] E. Dahlman, S. Parkvall, and J. Skold, *4G, LTE-advanced Pro and the Road to 5G*. Academic Press, 2016.

[2] R. S. E. Perahi, *Next Generation Wireless LANS*. New York, USA: Cambridge University Press, 2008.

[3] I.-T. Lu and K.-J. Tsai, "Channel estimation in a proposed IEEE802.11n OFDM MIMO WLAN system," in *Sarnoff Symposium, 2007 IEEE*, April 2007, pp. 1–5.

[4] S. Noh, Y. Sung, and M. D. Zoltowski, "A new precoder design for blind channel estimation in MIMO-OFDM systems," *IEEE Transactions on Wireless Communications*, vol. 13, no. 12, pp. 7011–7024, Dec 2014.

[5] L. Tong, G. Xu, and T. Kailath, "Blind identification and equalization based on second-order statistics: a time domain approach," *Information Theory, IEEE Transactions on*, vol. 40, no. 2, pp. 340–349, Mar 1994.

[6] C. Shin, R. W. Heath, and E. J. Powers, "Blind channel estimation for MIMO-OFDM systems," *IEEE Transactions on Vehicular Technology*, vol. 56, no. 2, pp. 670–685, March 2007.

[7] A. Ladaycia, A. Mokraoui, K. Abed-Meraim, and A. Belouchrani, "Performance bounds analysis for semi-blind channel estimation in MIMO-OFDM communications systems," *IEEE Transactions on Wireless Communications*, vol. 16, no. 9, pp. 5925–5938, 2017.

[8] K. Liu, J. P. C. L. da Costa, H. C. So, and A. L. F. de Almeida, "Semi-blind receivers for joint symbol and channel estimation in space-time-frequency MIMO-OFDM systems," *IEEE Transactions on Signal Processing*, vol. 61, no. 21, pp. 5444–5457, Nov 2013.

[9] G. Favier and A. L. F. de Almeida, "Tensor space-time-frequency coding with semi-blind receivers for MIMO wireless communication systems," *IEEE Transactions on Signal Processing*, vol. 62, no. 22, pp. 5987–6002, Nov 2014.

[10] Y. S. Cho, J. Kim, W. Y. Yang, and C. G. Kang, *MIMO-OFDM wireless communications with MATLAB*. John Wiley & Sons, 2010.

[11] S. M. Kay, "Fundamentals of statistical signal processing, volume I: Estimation theory (v. 1)," *PTR Prentice-Hall, Englewood Cliffs*, 1993.

[12] S. Fortunati, F. Gini, M. S. Greco, and C. D. Richmond, "Performance bounds for parameter estimation under misspecified models: Fundamental findings and applications," *IEEE Signal Processing Magazine*, vol. 34, no. 6, p. 142–157, 2017.

[13] H. White, "Maximum likelihood estimation of misspecified models," *Econometrica*, pp. 1–25, 1982.

[14] Q. H. Vuong, "Cramer-Rao bounds for misspecified models," *Caltech*, 1986.

[15] C. Gourieroux, A. Monfort, and A. Trognon, "Pseudo maximum likelihood methods: Theory," *Econometrica*, pp. 681–700, 1984.

[16] L. T. Thanh, K. Abed-Meraim, and N. L. Trung, "Misspecified Cramer-Rao bounds for blind channel estimation under channel order misspecification," *IEEE Trans. Signal Process.*, 2021.